DE GRUYTER OPEN

Journal of ELECTRICAL ENGINEERING, VOL 69 (2018), NO1, 39–45

Exact analytical modeling of magnetic vector potential in surface inset permanent magnet DC machines considering magnet segmentation

Ali Jabbari *

Surface inset permanent magnet DC machine can be used as an alternative in automation systems due to their high efficiency and robustness. Magnet segmentation is a common technique in order to mitigate pulsating torque components in permanent magnet machines. An accurate computation of air-gap magnetic field distribution is necessary in order to calculate machine performance. An exact analytical method for magnetic vector potential calculation in surface inset permanent magnet machines considering magnet segmentation has been proposed in this paper. The analytical method is based on the resolution of Laplace and Poisson equations as well as Maxwell equation in polar coordinate by using sub-domain method. One of the main contributions of the paper is to derive an expression for the magnetic vector potential in the segmented PM region by using hyperbolic functions. The developed method is applied on the performance computation of two prototype surface inset magnet segmented motors with open circuit and on load conditions. The results of these models are validated through FEM method.

K e y w o r d s: analytical modeling, surface inset PM motor, magnet segmentation, sub-domain method, FEM

1 Introduction

Permanent magnet motors are interested in industrial applications due to their high efficiency and power density [1, 2]. An accurate prediction of air-gap magnetic field distribution is necessary in order to calculate machine performance. A variety of techniques including analytical and numerical methods has been conducted to evaluate the magnetic vector potential in electrical machines. Numerical methods like finite element method (FEM) give accurate results and are time consuming specially in first step of design stage. Analytical methods including conformal mapping [3]-[6], Magnetic Equivalent Circuit (MEC) [7–9], sub-domain model [10–26] and slot relative permeance calculation [27–30] are reported to model electrical machines and are useful in first step of performance evaluation and design optimization stage. The sub-domain model is more accurate than the other analytical models [7]. This method is developed based on solution of Laplace and Poisson equations in different regions by applying boundary conditions for electrical machines [10–26].

To author's knowledge, a few analytical models are presented to calculate magnetic vector potential in surface inset permanent magnet motors [27–29]. No references in the literature addressing the issue of an analytical model for surface inset magnet segmented machines were found.

The focus of this paper is to develop an analytical model based on resolution of Laplace and Poisson equations in surface inset permanent magnet machines by using the sub-domain method considering magnet segmentation and slotting effects. It is shown that the developed model can effectively estimate magnetic vector potential, magnetic flux density, cogging torque and electromagnetic torque. This model is applied on the performance calculation of two prototypes, *ie* a 2 segmented 5S-2P PM motor and a 3 segmented 5S-2P PM motor. It is shown that the results of analytical model are in close agreement with the results of FEM.

2 Problem statement

The geometrical representation of the investigated permanent magnet motor with magnet segmented outer rotor layout is shown in Fig. 1. The machine model is divided into three sub-domains including the armature slots region (domain j) which has Q_1 slots, the air-gap region (domain I) and the permanent magnet region (domain k) which has Q_2 magnets. The machine parameters including the stator yoke radius R_1, the stator surface radius R_2, the rotor surface radius R_3, and the rotor slot radius R_4.

* Department of Mechanical Engineering, Faculty of Engineering, Arak University, Arak, 38156-8-8849, Iran, a-jabbari@araku.ac.ir

DOI: 10.1515/jee-2018–0005, Print (till 2015) ISSN 1335-3632, On-line ISSN 1339-309X © 2018FEI STU

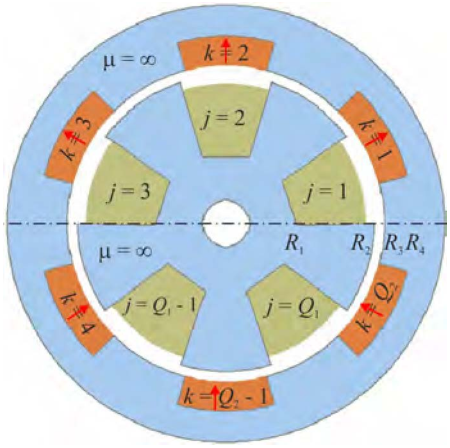

Fig. 1. Schematic representation of a surface inset magnet segmented motor

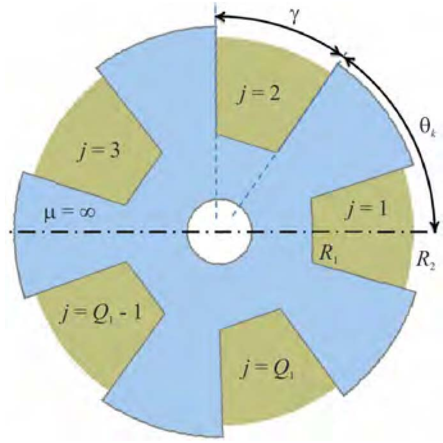

Fig. 2. Armature slot region (domain j) with its boundaries

The angular position of the j-th armature slot and k-th stator permanent magnet are defined as

$$\theta_j = -\frac{\alpha}{2} + \frac{2j\pi}{Q_1} \quad \text{with } 1 \le j \le Q_1\,, \tag{1}$$

$$\theta_k = -\frac{\gamma}{2} + \frac{2k\pi}{Q_2} \quad \text{with } 1 \le k \le Q_2\,. \tag{2}$$

3 Magnetic vector potential calculation

General solution of Laplace or Poisson equation in each sub-domain is developed in this section. The Laplace equation can be described in polar form as

$$\frac{\partial^2 A}{\partial r^2} + \frac{1}{r}\frac{\partial A}{\partial r} + \frac{1}{r^2}\frac{\partial^2 A}{\partial \theta^2} = 0 \quad \text{for} \quad \begin{cases} R_1 \le r \le R_2\,, \\ \theta_1 \le \theta \le \theta_2\,. \end{cases} \tag{3}$$

Replacing r by $R_1 e^{-t}$, one obtains

$$\frac{\partial^2 A}{\partial t^2} + \frac{\partial^2 A}{\partial \theta^2} = 0 \quad \text{for} \quad \begin{cases} \ln\frac{R_1}{R_2} \le t \le 0\,, \\ \theta_1 \le \theta \le \theta_2\,. \end{cases} \tag{4}$$

3.1 Magnetic vector potential in the armature slot sub-domain (Region j)

The Poisson equation in the armature slot sub-domain is given by

$$\frac{\partial^2 A_j}{\partial t^2} + \frac{\partial^2 A_j}{\partial \theta^2} = -\mu_0 J \quad \text{for} \quad \begin{cases} t_1 \le t \le t_2\,, \\ \theta_j \le \theta \le \theta_j + \alpha \end{cases} \tag{5}$$

where $t_1 = \ln\big(R_1/R_2\big)$ and $t_2 = 0$.

Neumann boundary conditions at the bottom and at each side of the slot are obtained as

$$\frac{\partial A_j}{\partial \theta}\Big|_{\theta=\theta_j} = 0 \quad \text{and} \quad \frac{\partial A_j}{\partial \theta}\Big|_{\theta=\theta_j+\alpha} = 0\,, \tag{6}$$

$$\frac{\partial A_j}{\partial t}\Big|_{t=t_2} = 0\,. \tag{7}$$

The general solution of (5) using the separation of variables method is given by

$$A_j(t,\theta) = a_0^j - \frac{1}{2}\mu_0 J_i \left(e^{-t_2}t + \frac{1}{2}e^{-2t+t_2}\right) + \sum_{h=1}^{\infty} \frac{\cosh\frac{h\pi}{\alpha}(t-t_2)}{\cosh\frac{h\pi}{\alpha}(t_1-t_2)} a_h^j \cos\frac{h\pi}{\alpha}(\theta-\theta_j) \tag{8}$$

where h is a positive integer and the coefficients a_0^j and a_h^j are determined based on the continuity and interface conditions.

The continuity of the magnetic vector potential between the sub-domain j and the region I leads to

$$A_j\,(t_1,\theta) = A_I\,(t_4,\theta) \quad \text{for} \quad \theta_j \le \theta \le \theta_j + \alpha \tag{9}$$

Interface condition (9) gives

$$a_0^j = \frac{1}{2}\mu_0 J_i \left(e^{-t_2}t + \frac{1}{2}e^{-2t+t_2}\right) + \frac{1}{\alpha}\int_{\theta_j}^{\theta_j+\alpha} A_I(t_4,\theta)\mathrm{d}\theta, \tag{10}$$

$$a_h^j = \frac{2}{\alpha}\int_{\theta_j}^{\theta_j+\alpha} A_I\,(t_4,\theta)\,.\cos\frac{h\pi}{\alpha}\,(\theta-\theta_j)\,\mathrm{d}\theta\,. \tag{11}$$

3.2 Magnetic vector potential in the air-gap sub-domain (Region I)

The Laplace equation in the air-gap sub-domain is given by

$$\frac{\partial^2 A_I}{\partial t^2} + \frac{\partial^2 A_I}{\partial \theta^2} = 0 \quad \text{for} \quad \begin{cases} t_3 \le t \le t_4\,, \\ 0 \le \theta \le 2\pi \end{cases} \tag{12}$$

where $t_3 = \ln(R_2/R_3)\,,\ t_4 = 0$.

The general solution of (12) considering periodicity boundary conditions is obtained as

$$A_I(t,\theta) = \sum_{n=1}^{\infty} \frac{1}{n}\Big(\frac{\cosh n(t-t_4)}{\sinh n(t_3-t_4)} a_n^I + \frac{\cosh n(t-t_3)}{\sinh n(t_4-t_3)} b_n^I\Big)\cos n\theta + \sum_{n=1}^{\infty} \frac{1}{n}\Big(\frac{\cosh n(t-t_4)}{\sinh n(t_3-t_4)} c_n^I + \frac{\cosh n(t-t_3)}{\sinh n(t_4-t_3)} d_n^I\Big)\sin n\theta. \tag{13}$$

The coefficients a_n^I, b_n^I, c_n^I and d_n^I are determined considering the continuity of magnetic vector potential between the internal air-gap sub-domain I and the region j and k using a Fourier series expansion of interface condition (14) and (15) over the air-gap interval.

The continuity of the magnetic vector potential between the internal air-gap sub-domain I and the regions j and k leads to

$$\frac{\partial A_I}{\partial t}\Big|_{t=t_3} = h(\theta) = \begin{cases} \frac{\partial A_k}{\partial t}\Big|_{t=t_6} & \text{for } \theta_k \le \theta \le \theta_k + \gamma\,, \\ 0 & \text{elsewhere,} \end{cases} \tag{14}$$

$$\frac{\partial A_I}{\partial t}\Big|_{t=t_4} = g(\theta) = \begin{cases} \frac{\partial A_j}{\partial t}\Big|_{t=t_1} & \text{for } \theta_j \le \theta \le \theta_j + \alpha\,, \\ 0 & \text{elsewhere.} \end{cases} \tag{15}$$

Interface condition (14) gives

$$a_n^I = \frac{2}{2\pi} \int_{\theta_k}^{\theta_k+\gamma} h(\theta) \cos n\theta \,\mathrm{d}\theta\,, \tag{16}$$

$$c_n^I = \frac{2}{2\pi} \int_{\theta_k}^{\theta_k+\gamma} h(\theta) \sin n\theta \,\mathrm{d}\theta\,. \tag{17}$$

Interface condition (15) gives

$$b_n^I = \frac{2}{2\pi} \int_{\theta_j}^{\theta_j+\alpha} g(\theta) \cos n\theta \,\mathrm{d}\theta\,, \tag{18}$$

$$d_n^I = \frac{2}{2\pi} \int_{\theta_j}^{\theta_j+\alpha} g(\theta) \sin n\theta \,\mathrm{d}\theta\,. \tag{19}$$

3.3 Magnetic vector potential in the stator permanent magnet sub-domain (Region k)

The Poisson equation in the stator permanent magnet sub-domain is given by

$$\frac{\partial^2 A_k}{\partial t^2} + \frac{\partial^2 A_k}{\partial \theta^2} = -\frac{\mu_0 e^t}{R_3}\Big(M_{\theta k} - \frac{\partial M_{rk}}{\partial \theta}\Big) \quad \text{for } \ t_5 \le t \le t_6\,,\ \theta_k \le \theta \le \theta_k + \gamma \tag{20}$$

where $t_5 = \ln(R_3/R_4)$ and $t_6 = 0$.

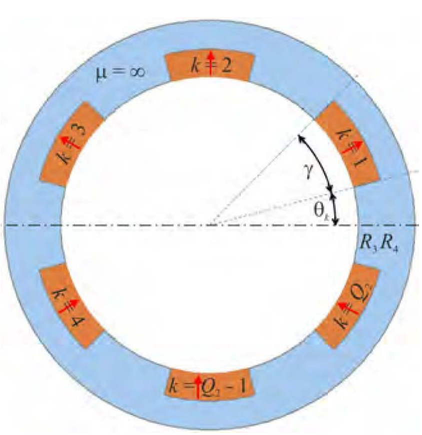

Fig. 3. Permanent magnet region (domain k) with its boundaries

The radial and tangential components of radial magnetization for inset design can be expressed as

$$M_{rk} = (-1)^{\left[\frac{k}{s+0.5}\right]} \frac{B_r}{\mu_0} \quad \text{with } k = 1,\ 2,\ \dots,\ Q_2, \tag{21}$$

$$M_{\theta k} = 0 \tag{22}$$

where p is number of pole pairs and s is number of magnet segmentations.

Neumann boundary conditions at the bottom and both sides of the permanent magnet slot are obtained as

$$\frac{\partial A_I}{\partial \theta}\Big|_{\theta=\theta_k} = f(t) = R_3 e^{-t} (-1)^{\left[\frac{k}{s+0.5}\right]} B_r\,, \tag{23}$$

$$\frac{\partial A_I}{\partial \theta}\Big|_{\theta=\theta_k+\gamma} = f(t) = R_3 e^{-t} (-1)^{\left[\frac{k}{s+0.5}\right]} B_r\,, \tag{24}$$

$$\frac{\partial A_I}{\partial t}\Big|_{t=t_5} = 0\,. \tag{25}$$

The general solution of (20) is

$$A_k(t,\theta) = a_0^k + R_3\big(e^{-(t-t_5)} + t\big)(-1)^{\left[\frac{k}{s+0.5}\right]} B_r\big(\theta - \theta_k - \frac{\gamma}{2}\big), \tag{26}$$

$$X_h^k = \begin{cases} \frac{4(-1)^{\left[\frac{k}{s+0.5}\right]} B_r}{\gamma z^2 (z^2-1)} & \text{if } h = 1, 3, 5, \dots \\ 0 & \text{if } h = 2, 4, 6, \dots \end{cases} \tag{27}$$

where $z = h\pi/\gamma$, h is a positive integer and the coefficients a_0^k and a_h^k are determined based on the continuity and interface conditions.

The continuity of the magnetic vector potential between the sub-domain k and the regions I leads to

$$A_k(t_6, \theta) = A_I(t_3, \theta) \quad \text{for } \ \theta_k \le \theta \le \theta_k + \gamma\,. \tag{28}$$

Interface condition (28) gives

$$a_0^k = R_2(-1)^{\left[\frac{k}{s+0.5}\right]} B_r\big(\theta - \theta_k - \frac{\gamma}{2}\big) + \frac{1}{\gamma} \int_{\theta_k}^{\theta_k+\gamma} A_I(t_3, \theta) \,\mathrm{d}\theta\,, \tag{29}$$

$$a_h^k = \frac{2}{\gamma} \int_{\theta_k}^{\theta_k+\gamma} A_I(t_3, \theta) \cos z(\theta - \theta_k) \,\mathrm{d}\theta\,. \tag{30}$$

4 Performance calculation and model evaluation

4.1 Performance computation

The electromagnetic torque is obtained using the Maxwell stress tensor and expressed as

$$T_e = \frac{L_s}{\mu_0} \int_0^{2\pi} BI_r(t_e, \theta)\, BI_\theta(t_e, \theta) \,\mathrm{d}\theta \tag{31}$$

where L_s is the axial length of the motor and

$$t_e = \ln \frac{R_2}{R_e}\,, \qquad R_e = (R_2 + R_3)/2\,. \tag{32}$$

Table 1. Parameters of the investigated 5s-2p motors

Symbol	Quantity	$S = 2$	$S = 3$
R_1	Inner radius of the armature slot	10 mm	10mm
R_2	Outer radius of the armature slot	16.4 mm	16.4mm
R_3	Inner radius of the stator PMs	17.4 mm	17.4mm
R_4	Outer radius of the stator PMs	20.5 mm	20.5mm
θ_j	Angular position of the first slot	17.5	17.5
θ_k	Angular position of the first PM	15	15
α	Slot opening angle	37	37
γ	PMs opening angle	60	30
p	Pole pairs-number	12	12
B_r	Remanence of the PMs	0.7 T	0.7T
L_s	Axial length	35 mm	35mm

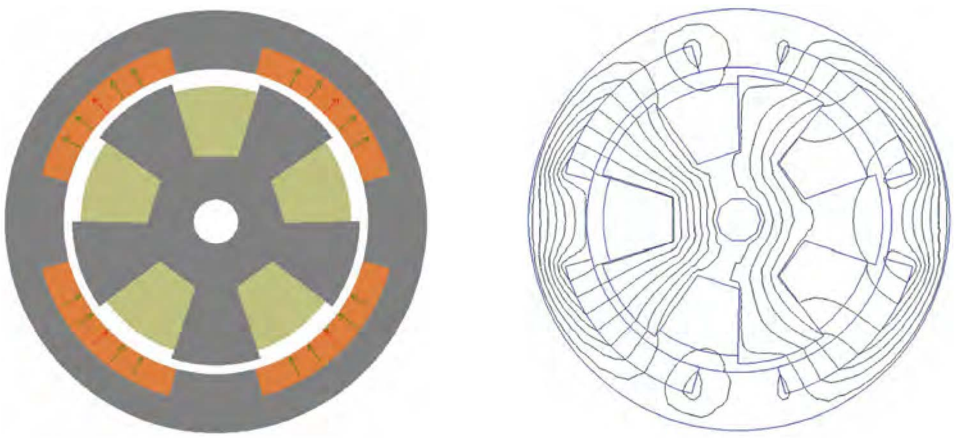

(a) (b)

Fig. 4. Two segmented surface inset PM motor: (a) – the schematic representation, (b) – magnetic flux distribution

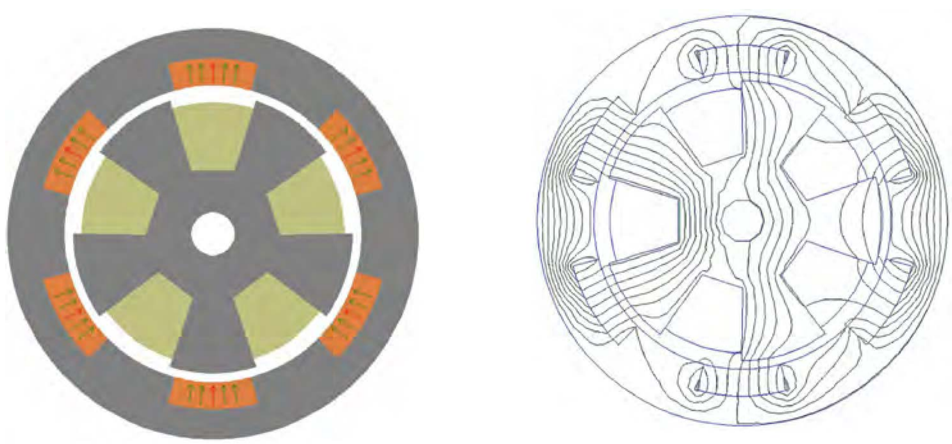

(a) (b)

Fig. 5. Three segmented surface inset PM motor: (a) – the schematic representation, (b) – magnetic flux distribution

4.2 Model evaluation

In this section, the proposed analytical model is used to study the open circuit and on load magnetic flux density, open circuit cogging torque and on load electromagnetic torque of two prototype motors. The results of analytical method are then verified by the results of finite element method. The motors parameters are given in Table 1. The schematic representation model of two investigated 5S-2P surface inset PM motors and their corresponding magnetic flux distribution obtained by FEA are shown in Fig. 4 and Fig. 5, respectively.

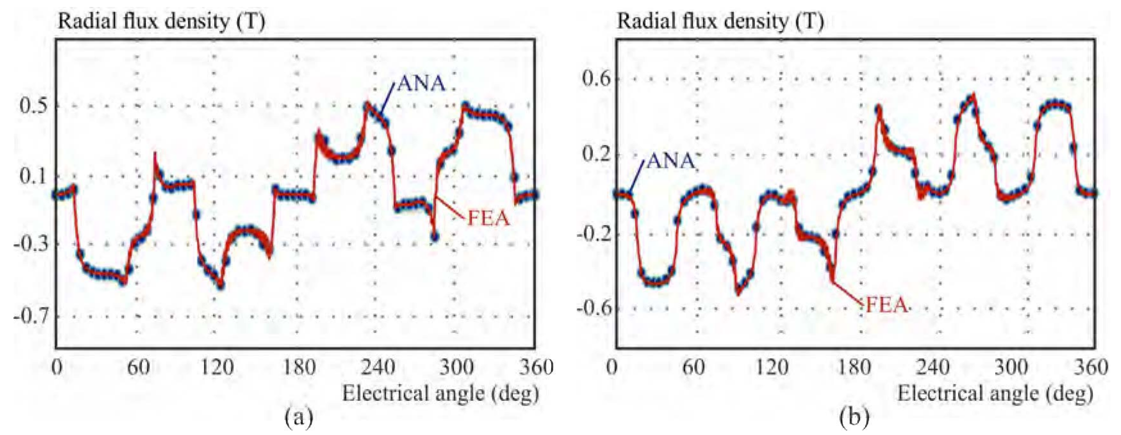

Fig. 6. No load analytical and numerical comparison of radial flux density for: (a) – 2 segment pm motor, (b) – 3 segment PM motor

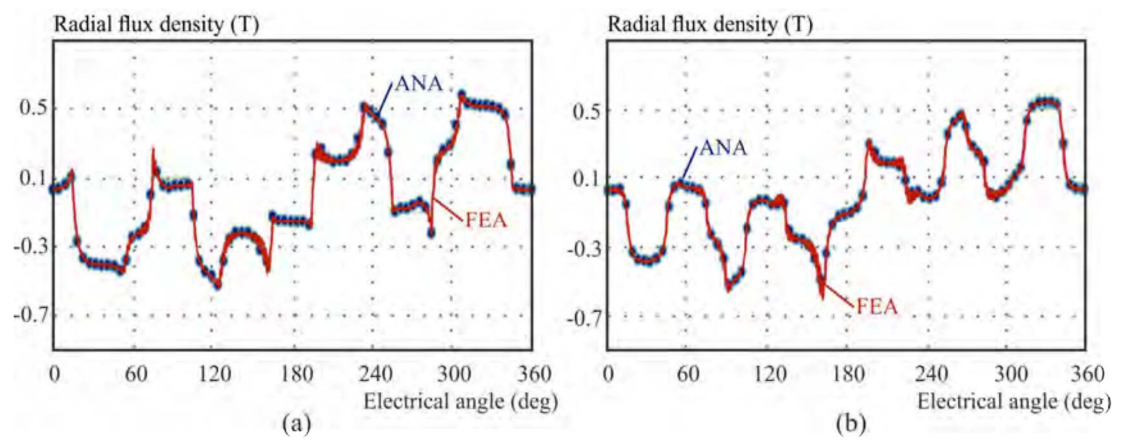

Fig. 7. On load analytical and numerical comparison of radial flux density for: (a) – 2 segment pm motor, (b) – 3 segment PM motor

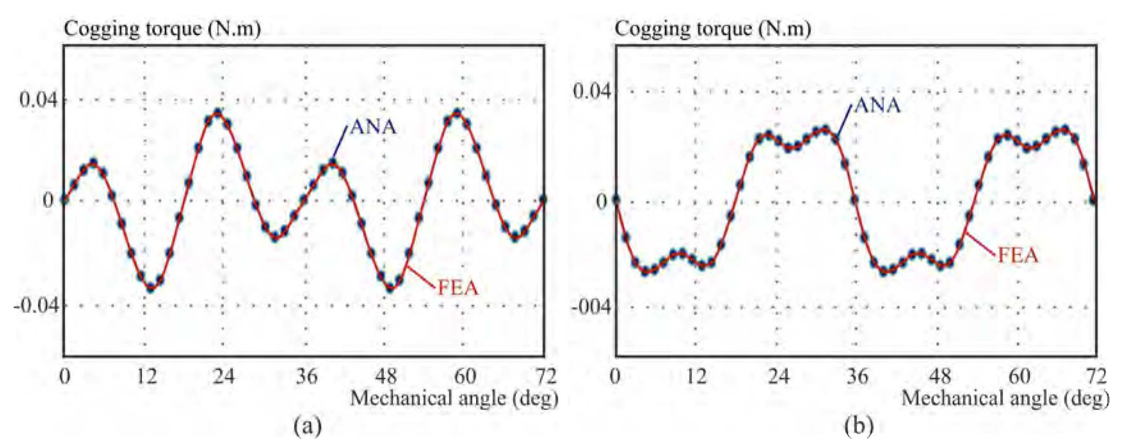

Fig. 8. Open circuit analytical and numerical comparison of cogging torque for: (a) – 2 segment pm motor, (b) – 3 segment PM motor

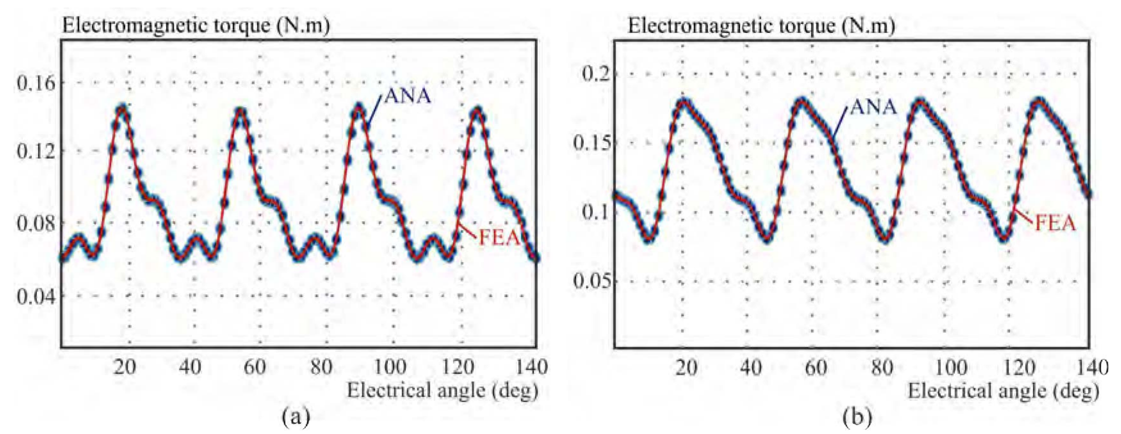

Fig. 9. On load analytical and numerical comparison of electromagnetic torque for: (a) – 2 segment pm motor, (b) – 3 segment PM motor

2D finite element method is applied on performance calculation of the two magnet segmented and three magnet segmented surface inset permanent magnet motors. A comparison of open circuit and on load analytical and numerical results of radial flux density, cogging torque and electromagnetic torque in the investigated motors are shown in Fig. 6, Fig. 7, Fig. 8 and Fig. 9, respectively.

5 Conclusion

An exact analytical model for performance prediction in surface inset permanent magnet machines considering slotting effects and magnet segmentation has been developed in this paper. Fourier analysis method based on subdomain method is applied to derive analytical expressions for calculation of magnetic vector potential, magnetic flux density, cogging torque and electromagnetic torque in surface inset permanent magnet machines. This model is applied for performance computation of two prototype motors and the results of proposed model are verified thanks to FEM results.

References

[1] A. Jabbari, M. Shakeri and S. A. Nabavi Naki, "Pole Shape Optimization of Permanent Magnet Synchronous Motors Using the Reduced Basis Technique", *Iranian J. of Electrical and Electronic Engineering*, 2010, vol. 6, no. 1, pp. 48–55.

[2] A. Jabbari, M. Shakeri and A. S. Gholamian, "Rotor Pole Shape Optimization of Permanent Magnet Brushless DC Motors Using the Reduced Basis Technique", *Advances Electrical and Computer Engineering*, 2009, vol. 9, no. 2, pp. 75–81.

[3] Z. Q. Zhu, D. Howe, "Instantaneous Magnetic Field Distribution Brushless Permanent Magnet DC Motors, III. Effect of Stator Slotting", *IEEE Trans. on Mag.* Jan 1993, vol. 29, no. 1, pp. 143–151.

[4] M. Markovic, M. Jufer and Y. Perriard, "Reducing the Cogging Torque Brushless DC Motors by Using Conformal Mappings", *IEEE Trans on Mag.* Mar 2004, vol. 40, no. 2, pp. 451–455.

[5] D. Zarko, D. Ban and T. A. Lipo, "Analytical Calculation of Magnetic Field Distribution the Slotted Air Gap of a Surface Permanent-Magnet Motor Using Complex Relative Air-Gap Permeance", *IEEE Trans. on Mag.* July 2006, vol. 42, no. 7, pp. 1828–1837.

[6] K. Boughrara, D. Zarko, R. Ibtiouen, O. Touhami and A. Rezzoug, "Magnetic Field Analysis of Inset and Surface-Mounted Permanent-Magnet Synchronous Motors Using Schwarz-Christoffel Transformation", *IEEE Trans. on Mag.* Aug 2009, vol. 45, no. 8, pp. 3166–3178.

[7] E. Ilhan, B. L. Gysen, J. J. Paulides and E. A. Lomonova, "Analytical Hybrid Model for Flux Switching Permanent Magnet Machines", *IEEE Trans. on Mag.* June 2010, vol. 46, no. 6, pp. 1762–1765.

[8] Y. Tang, T. E. Motoasca, J. J. Paulides and E. A. Lomonova, "Analytical Modeling of Flux-Switching Machines Using Variable Global Reluctance Networks", *Electrical Machines ICEM*, XXth International Conference on, 2012, Sep 2, pp. 2792–2798.

[9] W. Hua, G. Zhang, M. Cheng and J. Dong, "Electromagnetic Performance Analysis of Hybrid-Excited Flux-Switching Machines by a Nonlinear Magnetic Network Model", *IEEE Trans. on Mag.* Oct 2011, vol. 47, no. 10, pp. 3216–3219.

[10] G. Qishan and G. Hongzhan, "Effect of Slotting PM Electric Machines", *Electric machines and power systems*, Jan 1985, vol. 10, no. 4, pp. 273–284.

[11] A. Jabbari, "2D Analytical Modeling of Magnetic Vector Potential Surface Mounted and Surface Inset Permanent Magnet Machines", *Iranian J. of Electrical and Electronic Engineering*, Dec 2017, vol. 13, no. 4, pp. 362–373.

[12] N. Boules, "Prediction of No-load Flux Density Distribution Permanent Magnet Machines", *IEEE Trans. on Ind. Appl.* May 1985, no. 3, pp. 633–643.

[13] B. Ackermann and R. Sottek, "Analytical Modeling of the Cogging Torque Permanent Magnet Motors", *Electrical Engineering (Archiv fur Elektrotechnik)* , Mar 1995, vol. 78 no. 2, pp. 117–125.

[14] A. Radun, "Analytical Calculation of the Switched Reluctance Motor's Unaligned Inductance", *IEEE Trans. on Mag.* Nov 1999, vol. 35, no. 6, pp. 4473–4481.

[15] K. F. Rasmussen, J. H. Davies, T. J. Miller, M. I. McGelp and M. Olaru, "Analytical and Numerical Computation of Air-Gap Magnetic Fields Brushless Motors with Surface Permanent Magnets", *IEEE Trans. on Ind. Appl.* Nov 2000, vol. 36, no. 6, pp. 1547–1554.

[16] X. Wang, Q. Li, S, . Wang and Q. Li, "Analytical Calculation of Air-Gap Magnetic Field Distribution and Instantaneous Characteristics of Brushless DC Motors", *IEEE Trans. on energy conversion*, Sep 2003, vol. 18, no. 3, pp. 424–432.

[17] Z. J. Liu and J. T. Li, "Analytical Solution of Air-Gap Field Permanent-Magnet Motors Taking into Account the Effect of Pole Transition over Slots", *IEEE Trans. on Mag.* Oct 2007, vol. 43, no. 10, pp. 3872–3883.

[18] Z. J. Liu, J. T. Li and Q. Jiang, "An Improved Analytical Solution for Predicting Magnetic Forces Permanent Magnet Motors", *J. of Appl. Phys.* Apr 2008, vol. 103, no. 7, 07F135.

[19] Liu, ZJ, Li and JT, "Accurate Prediction of Magnetic Field and Magnetic Forces Permanent Magnet Motors using an Analytical Solution", *IEEE Trans. on Energy Conversion.* Sep 2008, vol. 23, no. 3, pp. 717–726.

[20] T. Lubin, S. Mezani and A. Rezzoug, "Exact Analytical Method for Magnetic Field Computation the Air Gap of Cylindrical Electrical Machines Considering Slotting Effects", *IEEE Trans. on Mag.* Apr 2010, vol. 46, no. 4, pp. 1092–1099.

[21] B. L. Gysen, E. Ilhan, K. J. Meessen, J. J. Paulides and E. A. Lomonova, "Modeling of Flux Switching Permanent Magnet Machines with Fourier Analysis", *IEEE Trans. on Mag.* June 2010, vol. 46, no. 6, pp. 1499–1502.

[22] K. Boughrara, R. Ibtiouen and T. Lubin, "Analytical Prediction of Magnetic Field Parallel Double Excitation and Spoke-Type Permanent-Magnet Machines Accounting for Tooth-Tips and Shape of Polar Pieces", *IEEE Trans. on Mag.* July 2012, vol. 48, no. 7, pp. 2121–2137.

[23] K. Boughrara, T. Lubin and R. Ibtiouen, "General Subdomain Model for Predicting Magnetic Field Internal and External Rotor Multiphase Flux-Switching Machines Topologies", *IEEE Trans. on Mag.* Oct 2013, vol. 49, no. 10, pp. 5310–5325.

[24] T. L. Tiang, D. Ishak and M. K. Jamil, "Complete Subdomain Model for Surface-Mounted Permanent Magnet Machines", *Energy Conversion CENCON*, 2014 IEEE Conference, 2014 Oct 13, pp. 140–145.

[25] X. Liu, H. Hu, J. Zhao, A. Belahcen, L. Tang and L. Yang, "Analytical Solution of the Magnetic Field and EMF Calculation Ironless BLDC Motor", *IEEE Trans.on Mag.* Feb 2016, vol. 52, no. 2, pp. 1–0.

[26] B. Dianati, H. Heydari and S. A. Afsari, "Analytical Computation of Air-Gap Magnetic Field a Viable Superconductive Magnetic Gear", *IEEE Trans. on Appl. Superconductivity.* Sep 2016, vol. 26, no. 6, pp. 1–2.

[27] F. M. Sargos and A. Rezzoug, "Analytical Calculation of Airgap Magnetic Field Produced by Inset Permanent Magnet Rotor Machine", *J. Physics III.* 1990, 1, pp. 103–110.

[28] Z. Q. Zhu, D. Howe and Z. P. Xia, "Prediction of Open-Circuit Airgap Field Distribution Brushless Machines having an Inset Permanent Magnet Rotor Topology", *IEEE Trans. on Mag.* Jan 1994, vol. 30, no. 1, pp. 98–107.

[29] A. Rahideh and T. Korakianitis, "Analytical Magnetic Field Distribution of Slotless Brushless Machines with Inset Permanent Magnets", *IEEE Trans. on Mag.* June 2011, vol. 47, no. 6, pp. 1763–1774.

[30] T. Lubin, S. Mezani and A. Rezzoug, "Two-Dimensional Analytical Calculation of Magnetic Field and Electromagnetic Torque for Surface-Inset Permanent-Magnet Motors", *IEEE Trans.on Mag.* June 2012, vol. 48, no. 6, pp. 2080–2091.

Received 17 June 2017

Ali Jabbari is an assistant professor in Mechanical Engineering Department at Arak University, Arak, Iran. He obtained a BSc degree in Mechanical Engineering from Iran University of Science and Technology in 2002. He received his MSc and PhD degrees both in Mechanical engineering from Mazandran University in 2004 and 2009, respectively. His research interests include renewable energy, electric machines, mechatronic systems and metal forming.